Optimal perturbations of non-parallel wakes and their stabilizing effect on the global instability

Gerardo Del Guercio,[1,2] Carlo Cossu,[1] and Gregory Pujals[2]
[1]*Institut de Mécanique des Fluides de Toulouse, CNRS and Université de Toulouse, Allée du Professeur Camille Soula, 31400 Toulouse, France*
[2]*PSA Peugeot Citroën, Centre Technique de Velizy, 2 Route de Gisy, 78943 Vélizy-Villacoublay Cedex, France*

We compute the spatial optimal energy amplification of steady inflow perturbations in a non-parallel wake and analyse their stabilizing action on the global mode instability. The optimal inflow perturbations, which are assumed spanwise periodic and varicose, consist in streamwise vortices that induce the downstream spatial transient growth of streamwise streaks. The maximum energy amplification of the streaks increases with the spanwise wavelength of the perturbations, in accordance with previous results obtained for the temporal energy growth supported by parallel wakes. A family of increasingly streaky wakes is obtained by forcing optimal inflow perturbations of increasing amplitude and then solving the nonlinear Navier-Stokes equations. We show that the linear global instability of the wake can be completely suppressed by forcing optimal perturbations of sufficiently large amplitude. The attenuation and suppression of self-sustained oscillations in the wake by optimal 3D perturbations is confirmed by fully nonlinear numerical simulations. We also show that the amplitude of optimal spanwise periodic (3D) perturbations of the basic flow required to stabilize the global instability is much smaller than the one required by spanwise uniform (2D) perturbations despite the fact that the first order sensitivity of the global eigenvalue to basic flow modifications is zero for 3D spanwise periodic modifications and non-zero for 2D modifications. We therefore conclude that first-order sensitivity analyses can be misleading if used far from the instability threshold, where higher order terms are the most relevant.

I. INTRODUCTION

Two-dimensional wakes behind bluff bodies support robust self-sustained vortex shedding for sufficiently large Reynolds numbers. The onset of self-sustained oscillations is associated to a global instability supported by a finite region of local absolute instability in the near wake.[1–3] There is a continued interest in controlling vortex shedding because, in addition to inducing unsteady loads on the body, it also leads to an increase of the mean drag.

Spanwise periodic (3D) perturbations of spanwise uniform (2D) wakes, e.g., obtained with periodic modulations of the trailing and/or leading edge of the bluff body[4–7] or spanwise periodic blowing and suction[8] can attenuate and even suppress vortex shedding and reduce the associated undesired drag and unsteady loads (see, e.g., Ref. 9 for a review). Recently, important progress has been made in the understanding of this stabilizing action from a linear stability perspective: Hwang *et al.*[10] show that appropriate 3D spanwise periodic perturbations of 2D absolutely unstable wake profiles lead to a reduction of the absolute growth rate. This reduction is observed for a range of spanwise wavelengths that is in accordance with experimental results, just as the fact that varicose perturbations are more stabilizing than sinuous ones. However, the question of the higher efficiency of 3D perturbations when compared to 2D ones in reducing the absolute growth rate was left partially open by this study. It is indeed known that lower rates of 3D blowing and suction, compared to 2D one, are required to suppress shedding in a cylinder wake.[8] This seems to contrast the fact that the

first-order sensitivity of the absolute instability growth rate with respect to 3D spanwise periodic modifications of the basic flow is zero,[10,11] therefore predicting that, at first order, 2D perturbations are more effective than 3D ones in reducing the absolute growth rate.

A partial explanation of the higher efficiency of 3D perturbations when compared to 2D ones has been given in another recent study[12] where we show that parallel "frozen" 2D wakes can support the large temporal amplification of streamwise streaks from stable spanwise periodic and streamwise uniform streamwise vortices via the lift-up effect.[13,14] The optimal perturbations leading to the optimal amplification of the streaks were computed and it was shown that varicose streaks of relatively small amplitude are able to completely quench the absolute instability.[12] It was also shown that the initial amplitude of optimal 3D perturbations necessary to quench the absolute instability is much smaller than the initial amplitude required by 2D perturbations.

Many questions were however left unanswered by the local temporal analysis developed in our previous investigation.[12] For instance, can optimal spatial amplifications be large in spatially diffusing wakes? The answer is not *a priori* clear because the wake diffusion not only reduces the basic flow shear fuelling the transient growth but also increases the local spanwise wavenumber of the perturbation, which is known from local analysis to reduce the growth. Another question is: are 3D optimal perturbations more efficient than 2D ones in stabilizing a *global* instability? The answer to this question is not obvious because finite downstream distances are needed to attain the maximum energy growth, while the pocket of absolute instability that needs to be controlled is located upstream, and therefore it is not clear how efficient optimal perturbations can be in quenching the absolute instability. The scope of the present study is to answer these questions by considering the *spatial* optimal perturbations and their influence on the *global* stability of *non-parallel* wakes.

An "artificial" wake, left free to spatially develop downstream the enforced inflow wake profile, is introduced as reference 2D basic flow in Sec. III. The use of such a basic flow allows us to find results which are independent of the specific body shape generating the wake and of the particular devices used to generate the optimal perturbations. The optimal spatial perturbations of this non-parallel wake are computed in Sec. IV following the procedure described in Sec. II. These optimal perturbations are defined as the perturbation profiles enforced at the inflow station that lead to the optimal energy amplification $G(x)$ at the downstream station x. This definition is quite different from that of optimal initial or inflow conditions leading to the optimal temporal energy amplification[15,16] $G(t)$. Optimal spatial energy amplifications have already been computed in non-parallel boundary layers by using direct-adjoint methods exploiting the parabolic nature of the boundary layer equations.[17,18] Here we choose to specifically design an alternative scalable optimization method (see Sec. II) that does not rely on the parabolic nature of the equations and that does not require the explicit computation of adjoint operators. The influence of forcing optimal perturbations on the global linear stability is investigated in Sec. V. The results of fully nonlinear simulations that validate these results in the nonlinear regime are reported in Sec. V D, while the used numerical methods are summarized in the Appendix.

II. PROBLEM FORMULATION

In this section the mathematical formulation of the analysis performed in the paper is briefly introduced. The formulation is general and can be applied to other non-parallel shear flows. Specific details about the particular wake profile and perturbations used in this study are mentioned in Secs. III–V.

A reference two-dimensional (2D) non-parallel plane basic flow $\mathbf{U}_{2D}(x, y)$ is obtained as a steady solution of the Navier-Stokes equations with inflow boundary condition $\mathbf{U} = U_0(y)\mathbf{e}_x$ given at $x = 0$ and free-stream conditions $\mathbf{U} \to U_\infty \mathbf{e}_x$ given as $y \to \pm\infty$. We denote by x, y, and z the streamwise, cross-stream, and spanwise coordinates and by $\mathbf{e}_x$, $\mathbf{e}_y$, $\mathbf{e}_z$ the associated unit vectors. The Reynolds number $Re = U^*_{ref}\delta^*/\nu$ is based on the characteristic velocity and length associated to $U_0(y)$ and on the kinematic viscosity ν of the fluid. The non-parallel basic flow $\mathbf{U}_{2D} = U(x, y)\mathbf{e}_x + V(x, y)\mathbf{e}_y$ is invariant to translations and reflections in the spanwise coordinate z (it is therefore two-dimensional or 2D).

Perturbations $\mathbf{u}'$ to the reference 2D basic flow are ruled by the Navier-Stokes equations in perturbation form:

$$\nabla \cdot \mathbf{u}' = 0, \tag{1}$$

$$\frac{\partial \mathbf{u}'}{\partial t} + (\nabla \mathbf{U})\,\mathbf{u}' + \left(\nabla \mathbf{u}'\right)\mathbf{U} + \left(\nabla \mathbf{u}'\right)\mathbf{u}' = -\nabla p' + \frac{1}{Re}\nabla^2 \mathbf{u}', \tag{2}$$

using $\mathbf{U} = \mathbf{U}_{2D}$ as basic flow.

In the first part of the study, dealing with optimal spatial perturbations of $\mathbf{U}_{2D}$, we consider steady perturbations $\mathbf{u}'$ of $\mathbf{U}_{2D}$ obtained by perturbing the inlet profile $U_0(y)$ with steady inflow perturbations $\mathbf{u}'_0(y, z)$. We are interested in steady perturbations both because they are spatially stable and because they are of interest in passive control applications. In particular, spanwise periodic perturbations of wavelength λ_z will be considered in the following. Considering small perturbations, the nonlinear term $(\nabla \mathbf{u}')\mathbf{u}'$ can be neglected, which makes the perturbation equations linear. Defining the local perturbation kinetic energy density as

$$e'(x) = \frac{1}{2\delta\lambda_z}\int_{-\infty}^{\infty}\int_{0}^{\lambda_z} \mathbf{u}' \cdot \mathbf{u}'\, dy\, dz, \tag{3}$$

the optimal spatial energy amplification of inflow perturbations is defined as

$$G(x) = \max_{\mathbf{u}'_0} \frac{e'(x)}{e'_0}. \tag{4}$$

Different approaches can be used to compute $G(x)$ and the associated optimal inflow perturbation. We choose here to decompose the inlet perturbation on a set of linearly independent functions $\mathbf{b}_0^{(m)}$, in practice limited to M terms, as

$$\mathbf{u}'_0(y, z) = \sum_{m=1}^{M} q_m \mathbf{b}_0^{(m)}(y, z). \tag{5}$$

Denoting by $\mathbf{b}^{(m)}(x, y, z)$ the perturbation velocity field obtained using $\mathbf{b}_0^{(m)}(y, z)$ as inlet perturbation, from the linearity of the operator follows that

$$\mathbf{u}'(x, y, z) = \sum_{m=1}^{M} q_m \mathbf{b}^{(m)}(x, y, z), \tag{6}$$

where the coefficients q_m are the same used in Eq. (5). The optimization problem in Eq. (4) can therefore be recast in terms of the M-dimensional control vector $\mathbf{q}$ as

$$G(x) = \max_{\mathbf{q}} \frac{\mathbf{q}^T \mathbf{H}(x)\mathbf{q}}{\mathbf{q}^T \mathbf{H}_0 \mathbf{q}}, \tag{7}$$

where the components of the symmetric matrices $\mathbf{H}(x)$ and $\mathbf{H}_0$ are

$$H_{mn}(x) = \frac{1}{2\delta\lambda_z}\int_{-\infty}^{\infty}\int_{0}^{\lambda_z} \mathbf{b}^{(m)}(x, y, z) \cdot \mathbf{b}^{(n)}(x, y, z)\, dy\, dz, \tag{8}$$

$$H_{0,mn} = \frac{1}{2\delta\lambda_z}\int_{-\infty}^{\infty}\int_{0}^{\lambda_z} \mathbf{b}_0^{(m)}(y, z) \cdot \mathbf{b}_0^{(n)}(y, z)\, dy\, dz. \tag{9}$$

Within this formulation $G(x)$ is easily found as the largest eigenvalue μ_{max} of the generalized $M \times M$ eigenvalue problem $\mu \mathbf{H}_0 \mathbf{w} = \mathbf{H}\mathbf{w}$. The corresponding eigenvector is the optimal set of coefficients $\mathbf{q}^{(opt)}$ maximizing the kinetic energy amplification at the selected streamwise station x. The corresponding inlet perturbation is $\mathbf{u}'^{(opt)}_0(y, z) = \sum_{m=1}^{M} q_m^{(opt)} \mathbf{b}_0^{(m)}(y, z)$. In the limit $M \to \infty$ the approximated solution converges to the exact solution.

In the second part of the study, the influence of forcing finite amplitude optimal perturbations on linear global stability is investigated. A family of 3D streaky nonlinear non-parallel basic flows

$\mathbf{U}_{3D}(x, y, z; A_0)$ is obtained by looking for steady solutions of the (nonlinear) Navier-Stokes equations with inflow boundary condition $\mathbf{U}_0(y, z) = U_0(y)\mathbf{e}_x + A_0\mathbf{u}'^{(opt)}_0(y, z)$ given at $x = 0$. $\mathbf{u}'^{(opt)}_0$ is normalized to unit x-local energy so that $e'(0) = A_0^2$ for $\mathbf{u}' = \mathbf{U}_{3D} - \mathbf{U}_{2D}$ (see the definition of e' in Eq. (3)). In general, it is not guaranteed that the linear optimal perturbations are also (nonlinearly) optimal at finite amplitude. However, for the present purpose of open-loop control, this is not a problem as long as they are still largely amplified. Using strictly optimal perturbations is also not critical because it is not likely that strictly optimal perturbations can be forced in a real flow and there is no guarantee that they would be also the optimal ones in reducing the global mode growth rate. The global linear stability of the $\mathbf{U}_{3D}$ basic flows is then analysed by integrating in time the linearized form of the Navier-Stokes equations (1) and (2) in perturbation form with $\mathbf{U} = \mathbf{U}_{3D}$. After the extinction of transients, the leading global mode emerges inducing an exponential growth or decay of the solution. The global growth rate is then deduced from the slope of the global energy amplification curve.

III. NON PARALLEL 2D REFERENCE WAKE

The 2D reference wake is computed by enforcing as inflow boundary condition the following well studied[2] wake profile:

$$U_0(y) = 1 + \Lambda\left[\frac{2}{1 + \sinh^{2N}(y \sinh^{-1} 1)} - 1\right], \tag{10}$$

with $\Lambda = (U_c^* - U_\infty^*)/(U_\infty^* + U_c^*)$, where U_c^* is the centreline and $U_\infty{}^*$ the freestream velocity (dimensional variables are starred). The velocity U_0 is made dimensionless with respect to the reference velocity $U_{ref}^* = (U_c^* + U_\infty^*)/2$. The spatial coordinates are made dimensionless with respect to the reference length δ_0^* that is the distance from the centreline to the point where the 2D wake velocity is equal to U_{ref}^*, computed at the inflow. We set $\Lambda = -1.35$ to ensure a small recirculation in the upstream region of the wake. For $\Lambda = -1.35$, the wake is globally unstable when $Re \gtrsim 39$ (not shown). In the following we will consider the value $Re = 50$ for which numerical simulation (see the Appendix for the numerical details) shows strong self-sustained oscillations in the wake (see Fig. 1(b)). As at $Re = 50$ the only unstable global mode is sinuous (antisymmetric with respect to the $y = 0$ axis), the unstable basic flow $\mathbf{U}_{2D}$ is computed by direct temporal integration by enforcing the y-symmetry of the solutions (otherwise a Newton-based continuation method would have been required). The reference basic flow is shown in Fig. 1(a). It can be seen how the basic flow vorticity, which is maximum at $x = 0$ with peaks at $y \approx \pm 1$, slowly diffuses downstream.

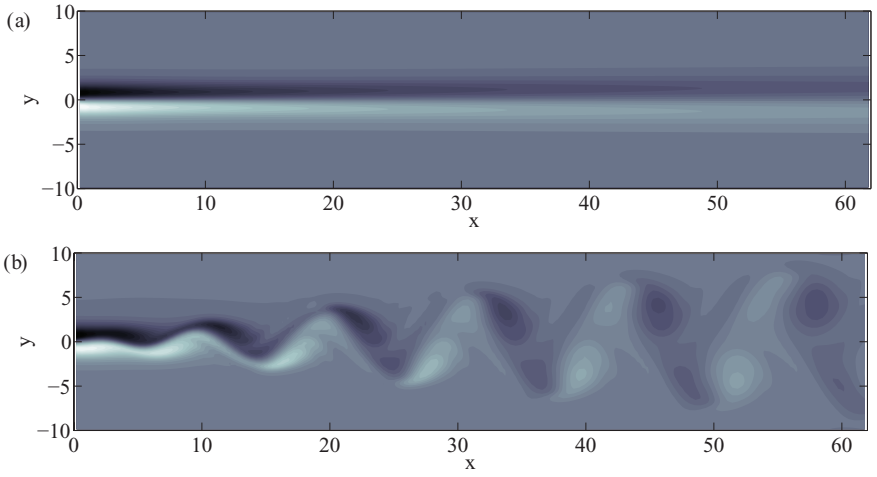

FIG. 1. Spanwise vorticity fields $\omega_z(x, y)$ associated to the reference 2D non-parallel wake at $Re = 50$. (a) (unstable) Basic 2D flow profile obtained by enforcing the y-symmetry of the solution. (b) Snapshot of the periodic self-sustained state obtained without enforcing the y-symmetry of the solution.

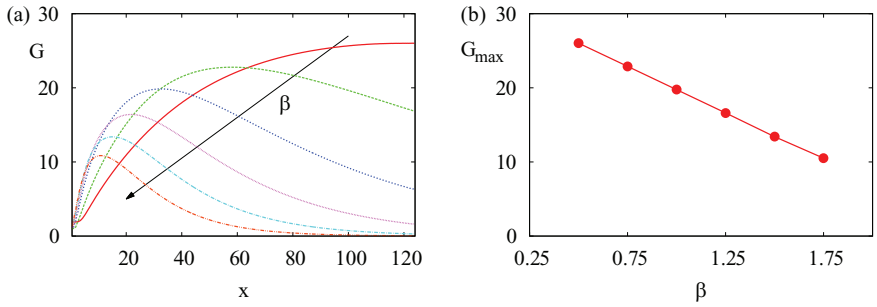

FIG. 2. Optimal spatial energy growths $G(x)$ (panel (a)) computed for the spanwise wavenumbers $\beta = 0.5, 0.75, \ldots, 1.50, 1.75$ at $Re = 50$ (outer to inner). The dependence $G_{max}(\beta)$ of the maximum energy growths on the spanwise wavenumber is reported in panel (b).

IV. OPTIMAL SPATIAL ENERGY GROWTH

Optimal steady inlet perturbations of $\mathbf{U}_{2D}$ maximizing the spatial energy amplification $G(x)$ are computed following the procedure described in Sec. II. Our previous investigation of the optimal temporal energy growth in parallel wakes[12] has shown that the most amplified spanwise periodic and streamwise uniform (corresponding to steady in our spatial framework) perturbations consist in streamwise vortices inducing the growth of streamwise streaks. We therefore consider inlet conditions of the type: $\mathbf{u'}_0 = (u'_0, v'_0, w'_0) = (0, \partial\psi/\partial z, -\partial\psi/\partial y)$. Single-harmonic spanwise periodic perturbations can be considered without loss of generality: $\psi' = f(y)\sin(\beta z)$. As varicose perturbations (mirror-symmetric with respect to the $y = 0$ plane) are the most efficient for control,[9,10,12] even if they are slightly less amplified than sinuous ones,[12] we enforce $f(-y) = -f(y)$ which leads to varicose streaks. The set of linearly independent inflow conditions used in Eq. (5) is chosen as $\mathbf{b}_0^{(m)}(y, z) = (0, \partial\psi^{(m)}/\partial z, -\partial\psi^{(m)}/\partial y)$ with $\psi^{(m)} = f_m(y)\sin(\beta z)$ and $f_m(y) = -f_m(y)$ for $m = 1, \ldots, M$. We have found well suited the set $f_m(y) = \sin(2m\pi y/L_y)$, where the numerical box extends from $-L_y/2$ to $L_y/2$ in the y direction.

Optimal energy growths have been computed for a set of spanwise wavenumbers β increasing M until a precision of 1% or higher on G_{max} was achieved (see also the Appendix for the numerical details of the computations). The computed optimal energy growth curves $G(x, \beta)$ are reported in Fig. 2(a). It is seen how, consistently with results form the local analysis,[12] both the maximum growth $G_{max} = \max_x G(x)$ and the position x_{max} where it is attained increase with increasing spanwise wavelength $\lambda_z = 2\pi/\beta$, i.e. with decreasing β (see also panel (b) of the same figure). The convergence of the optimal growth curves with increasing M is quite fast, and this for all the considered values of β, as can be seen in Fig. 3. Well converged results, with relative variations below 1% are obtained with only $M = 16$ terms.

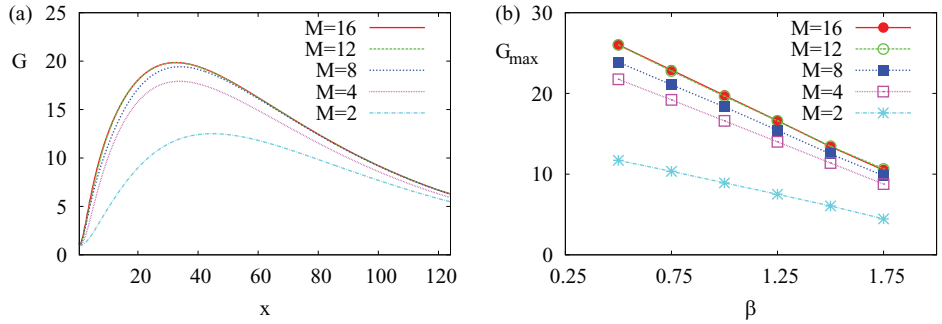

FIG. 3. Convergence of the optimal energy growth $G(x)$ for $\beta = 1$ (panel (a)) and of the maximum energy growth $G_{max}(\beta)$ (panel (b)) when the number M of linearly independent inflow conditions is increased at $Re = 50$. Well converged results are obtained for $M = 16$.

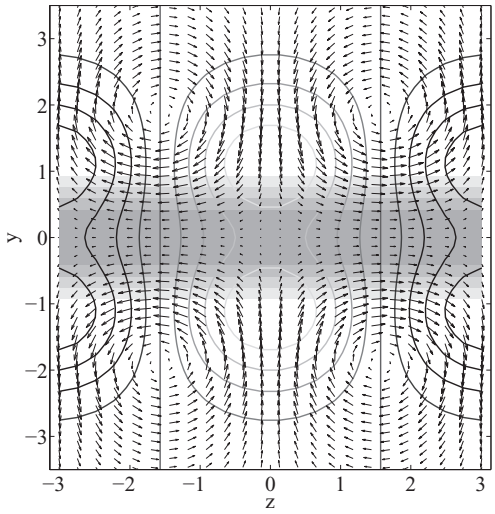

FIG. 4. Cross-stream (y-z) view of the cross-stream v_0'-w_0' components of optimal vortices (arrows) forced at the inflow ($x = 0$) and of the streamwise u' component of the corresponding optimal streaks (contour-lines) at $x = x_{max}$ for $Re = 50$, $\beta = 1$. The 2D basic flow wake streamwise velocity at the inflow $U_0(y)$ is also reported in grey-scale with white corresponding to the freestream velocity and dark grey the minimum velocity (wake centreline).

The optimal inflow perturbations ($x = 0$) and the maximum response ($x = x_{max}$) associated to the maximum growth G_{max} obtained for $\beta = 1$ are reported in Fig. 4. The corresponding velocity profiles are reported in Fig. 5, where additional values of β are also considered. The optimal inflow perturbations consist in two rows of counter-rotating vortices on each side of the $y = 0$ plane, with opposite rotation on each side. These vortices induce the growth of y-symmetric (varicose) streaks. From Fig. 5 it can be seen how, for increasing spanwise wavelengths λ_z (decreasing β), the size of optimal perturbations increases in the normal (y) direction (and of course also in the spanwise z direction).

The observed trends are in agreement with those found in our previous local analysis.[12] However, the maximum spatial growth rates obtained in the non-parallel case are smaller than the temporal ones obtained at the same nominal β under the frozen and parallel flow approximation. This is not surprising because the nominal values of β and Re of the non-parallel results are based on the properties of the wake profile at the inflow ($x = 0$). As the dimensional reference length $\delta^*(x)$ (the y^*

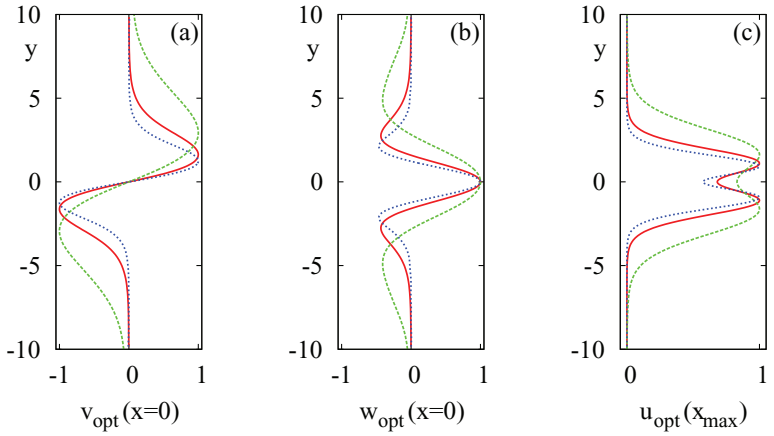

FIG. 5. Normalized amplitude of the $v(x = 0, y, z = 0)$ component (panel (a)) and $w(x = 0, y, z = \lambda_z/4)$ components (panel (b)) of the optimal inflow boundary vortices. The normalized amplitude of the $u(x = x_{max}, y, z = 0)$ streamwise component of the corresponding optimally amplified streaks is plotted in panel (c). Three selected spanwise wavenumbers are considered: $\beta = 0.5$ (dashed line, green), $\beta = 1$ (solid line, red), and $\beta = 1.5$ (dotted line, blue).

value where $U^*_{2D}(y^*) = U^*_{ref}$) increases with x, a dimensionless wavenumber $\beta = \beta^*\delta^*$ based on the local scale would increase going downstream. As the maximum growth rate is a decreasing function of β, it is not surprising that the maximum growth rates are smaller than the ones that would be obtained if the wake was parallel. Therefore, the results of the present analysis should be compared to the ones of the local analysis obtained at larger values of β.

V. STABILIZING EFFECT OF OPTIMALLY FORCED STREAKS ON GLOBAL MODES

In this second part of the study, we investigate the influence of the forcing of optimal perturbations on the linear global stability of the wake. The input parameter of this analysis is the amplitude A_0 of the forcing at the inflow boundary and the output is the linear growth rate s_r of the global mode supported by the streaky wake. All the results are obtained for $Re = 50$ and $\beta = 1$. The choice of $\beta = 1$ is not completely arbitrary. On the one hand, in order to obtain large energy amplifications, one should choose low values of β. For low β, however, not only would the cross-stream size of the inlet optimal vortices be probably too large to be implemented in practical applications but, even more importantly, large amplitudes of the streaks would be obtained only far downstream (e.g., $x_{max} \approx 120$ for $\beta = 0.5$). This is a problem because the main scope of the control is to reduce the absolute growth rate in the absolute region which extends up to $x \approx 5$. On the other hand, selecting large values of β, in order to have x_{max} in the absolute region, would lead to poor energy amplifications and would exclude any damping in the convective region. The value $\beta = 1$ is a good compromise between these two extrema. In particular, as can be seen from Fig. 2(a), the obtained $G(x)$ for $\beta = 1$ in the region $x \lesssim 10$ are sensibly the same of those obtained for higher β.

A. Streaky wakes basic flows

Non-parallel streaky (3D) wake basic flows $\mathbf{U}_{3D}(x, y, z; A_0)$ are computed by enforcing at $x = 0$ the inflow condition $\mathbf{U} = U_0(y)\mathbf{e}_x + A_0\mathbf{u}'^{(opt)}_0$ and by then computing the corresponding steady solution of the (nonlinear) Navier-Stokes equations, as explained in Sec. II. The solution, which may be unstable, is obtained by enforcing symmetry with respect to the $y = 0$ plane, exactly as done to compute $\mathbf{U}_{2D}$. The local amplitude of the streaks is measured extending the standard definition used in previous studies:[12,19]

$$A_s(x) = \frac{1}{2}\frac{\max_{y,z}\left(U_{3D} - U_{2D}\right) - \min_{y,z}\left(U_{3D} - U_{2D}\right)}{\max_y U_0 - \min_y U_0}. \tag{11}$$

In this definition the streak amplitude at the station x is defined as half the maximum deviation of the streaky 3D profile from the reference 2D profile, at the same x station, normalized by the maximum velocity variation of the inflow 2D reference profile.

The considered values of A_0 and the obtained values of A_s at x_{max} (maximum value of A_s) and in the middle of the absolute instability region ($x = 2.7$) are reported in Table I, where each considered case is given a literal label. Case A corresponds to the reference two-dimensional wake profile $\mathbf{U}_{2D}$ (no streaks) while cases B, C, D, and E are obtained by increasing the inlet amplitude A_0 of the forced optimal perturbations. The nonlinear streaks amplitude evolution $A_s(x)$ associated to the velocity fields $\mathbf{U}_{3D}$ are reported in Fig. 6(a) for the considered cases. From Fig. 7, where streaky basic flows are shown in the symmetry plane $y = 0$, it is seen how, indeed for increasing A_0, the wake is increasingly 3D. The effect of nonlinearity is to slightly reduce the maximum energy growth (from ≈20 in the linear small amplitude limit to ≈17–15 for streaks D and E, not shown) and to induce a mean flow distortion that slightly counteracts the effect of the streaks.

B. Linear global stability analysis

The linear global stability analysis is performed via a direct numerical simulation of the Navier-Stokes equations (1) and (2) linearized upon the 3D streaky basic flows $\mathbf{U}_{3D}$ defined above (Sec. V A). In previous local stability analyses[10,12] it was shown that for large streaks amplitudes,

TABLE I. Considered nonlinear streaky wake basic flows. A_0 is the finite amplitude given, at the inflow, to the linear optimal boundary perturbations (vortices). $A_{s,max}$ is the maximum streak amplitude reached in the nonlinear numerical simulation. Case A corresponds to the reference two-dimensional wake. Cases B, C, D, and E are obtained by increasing A_0.

Case	A_0	$A_{s,max}$ (%)	$A_s(x = 2.7)$ (%)
A	0.000	0	0
B	0.057	10.3	2.5
C	0.085	15.1	3.7
D	0.120	20.4	5.2
E	0.171	27.3	7.4

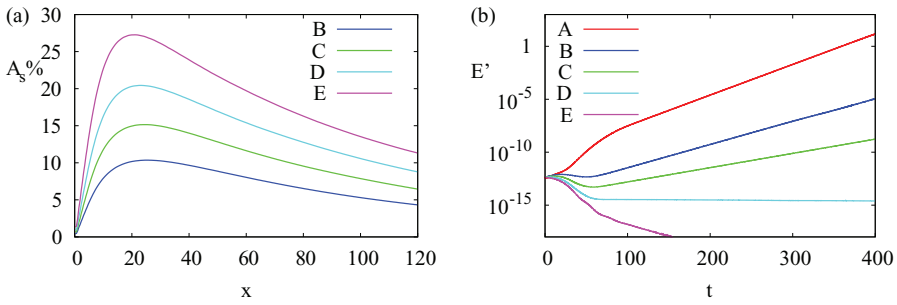

FIG. 6. Spatial evolution of the streaks amplitudes $A_s(x)$ for increasing amplitudes A_0 of the inflow optimal perturbations (panel (a)) and temporal evolution of the global kinetic energy of secondary perturbations $E'(t)$ to the considered reference and streaky basic flows (panel (b)). All the results have been obtained for $Re = 50$ and $\beta = 1$.

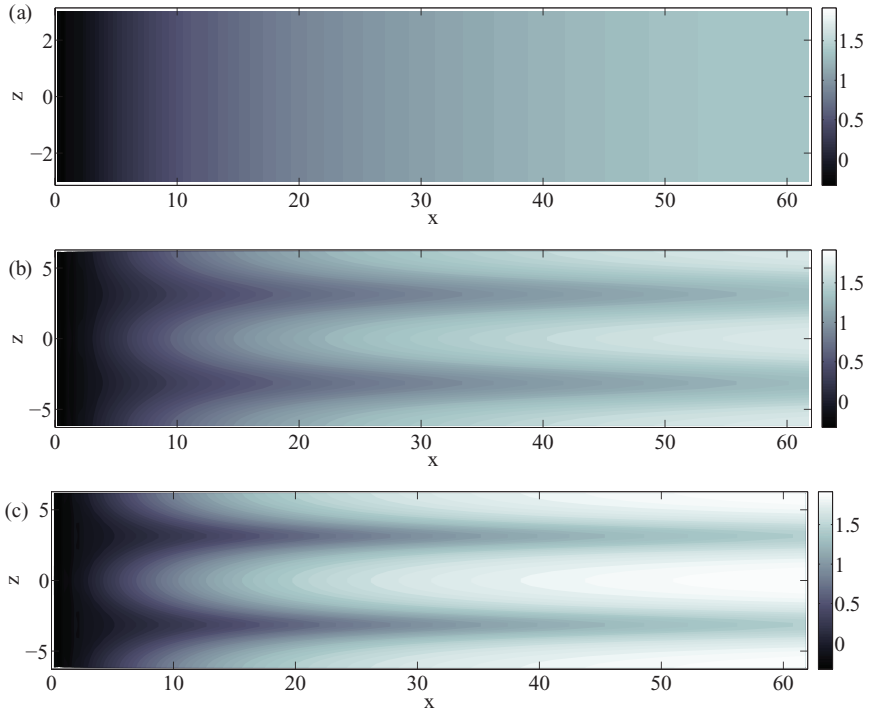

FIG. 7. Streaky basic flows. Distribution of the streamwise velocity $u(x, y = 0, z)$ in the $y = 0$ symmetry plane. The reference 2D case A is reported in panel (a), while cased C and E, obtained by increasing the amplitude A_0 of the inflow optimal perturbations, are reported in panels (b) and (c), respectively.

the dominant absolute mode is subharmonic, i.e., its spanwise wavelength is twice that of the basic flow streaks. This is taken in due consideration by integrating the linearized equations in a domain including two basic flow streaks wavelengths ($L_z = 2\lambda_z$). Noisy initial conditions on $\mathbf{u}'$ are given for the reference 2D wake (case A). The unstable global mode emerging for large times in the reference 2D wake is then used, upon normalization of its amplitude, as initial condition on $\mathbf{u}'$ in simulations with the increasingly streaky basic flows B,...,E.

The temporal evolution of the global perturbation kinetic energy

$$E' = \frac{1}{2\delta L_x L_z} \int_0^{L_x} \int_{-L_y/2}^{L_y/2} \int_0^{L_z} \mathbf{u}' \cdot \mathbf{u}' \, dx \, dy \, dz$$

is reported in Fig. 6(b). After an initial transient extending to $t \approx 70$, the dependence of E' on time is exponential (a straight line in the lin-log scales used in the figure), where the rate of growth or of decay is twice the growth rate of the global mode.

As anticipated (see, e.g., Fig. 1(b)) the reference 2D wake (case A) is strongly linearly unstable at $Re = 50$. The forcing of 3D linearly optimal perturbations of increasing amplitude has a stabilizing effect on the global instability. The growth rate first reduced for low amplitude streaks (cases B and C) is then rendered quasi-neutral (case D) and finally completely stable for sufficiently large streak amplitudes (case E).

In the neutral and stable case the streaks amplitudes $A_s(x = 2.7)$, measured in the middle of the absolute instability region of the reference 2D wake, are respectively of $\approx$5% and $\approx$7%. These values are not far from the $\approx$8% value at which the absolute instability was completely quenched in our previous local stability analysis.[12] Also remark that, in the present non-parallel case A_s is given in terms of the entrance reference maximum $\Delta U_{2D}(x = 0)$, but if it was based on the local value of $\Delta U_{2D}(x)$ which is decreased with x, this would result in even larger downstream values of A_s. The stabilization of the global mode therefore appears to be associated to a strong reduction of the pocket of absolute instability that drives the global mode oscillations in the 2D reference case. A local stability analysis of the basic flow profiles extracted at $x = 2.7$ (not shown) indeed confirms that the local absolute growth rate is reduced with increasing streak amplitudes and that it is completely quenched by streak E.

C. Sensitivity of the global growth rate to the amplitude of 3D optimal structures

1. The first order sensitivity of the global growth rate to streaks is zero

In previous studies based on local stability analyses,[10,11] it was shown that the sensitivity of the absolute growth rate to 3D spanwise periodic modifications of the basic flow is zero. The argument developed in the local absolute instability analysis is easily extended to the global stability analysis of the nonparallel wake and proceeds as follows. Denote by $\mathbf{L}_{2D}$ the Navier-Stokes operator linearized near the 2D basic flow $\mathbf{U}_{2D}$. For small values of the inflow amplitude of optimal perturbations, the basic flow is modified by a small amount $\delta\mathbf{U} = \mathbf{U}_{3D} - \mathbf{U}_{2D}$ that induces a small change $\delta\mathbf{L}$ in the linear operator. At first order, the change of the leading eigenvalue induced by this small variation is[20,21] $\delta s = \langle \mathbf{w}_{2D}^\dagger, \delta\mathbf{L}\mathbf{w}_{2D} \rangle / \langle \mathbf{w}_{2D}^\dagger, \mathbf{w}_{2D} \rangle$, where $\mathbf{w}_{2D}$, s_{2D}, $\mathbf{w}_{2D}^\dagger$ are, respectively, the leading global mode, eigenvalue, and adjoint global mode associated to $\mathbf{U}_{2D}$, and the standard inner product is defined as $\langle \mathbf{a}, \mathbf{b} \rangle = \int_0^{L_x} \int_{-L_y/2}^{L_y/2} \int_0^{L_z} \mathbf{a} \cdot \mathbf{b} \, dx \, dy \, dz$. From Eq. (2) it is seen that the variation $\delta\mathbf{L}$ induced by $\delta\mathbf{U}$ consists only in spanwise periodic terms as $\delta\mathbf{U}$ is itself spanwise periodic. As $\mathbf{w}_{2D}$ and $\mathbf{w}_{2D}^\dagger$ do not depend on z, it follows[22] that $\langle \mathbf{w}^\dagger, \delta\mathbf{L}\mathbf{w} \rangle = 0$ and therefore that $\delta s = 0$. This is not the case for 2D (spanwise uniform) perturbations of $\mathbf{U}$ for which the variation of the leading eigenvalue is, in general, non-zero.

2. Effective sensitivity of global growth rate to spanwise periodic basic flow modifications and comparison with 2D modifications

We now consider the observed dependence of the most unstable global mode on the control amplitude. Such a control amplitude is unequivocally defined in terms of inflow optimal perturbation

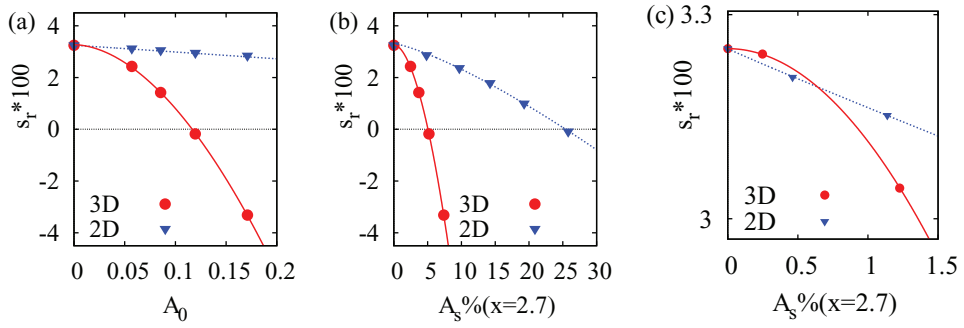

FIG. 8. Dependence of the growth rate of the global eigenvalue s_r on the inflow optimal perturbation amplitude A_0 (panel (a)) and on the streak amplitude $A_s(x = 2.7)$ measured in the centre of the absolute region of the reference 2D wake (panels (b) and (c) for a zoomed plot). A spanwise uniform perturbation (2D) has been also considered for comparison. Symbols denote data points, while lines are best fits to the data points.

amplitudes A_0. The dependence of the global growth rate s_r on the inflow optimal perturbation amplitude A_0 is displayed in Fig. 8(a). If this dependence is also to be reported in term of streaks amplitudes, for the considered streaks with $\beta = 1$, it makes no sense to report it in terms of $A_{s,max}$ because this value is attained far downstream, in the convectively unstable region. We instead take as an indicator of the "useful" streak amplitude the amplitude of the streaks in the middle of the absolute region of the unperturbed flow $A_s(x = 2.7)$. The dependence of s_r on this amplitude is reported in Fig. 8 (panels (b) and (c) for a zoom).

In the same figures the variation of the growth rate s_r induced by a 2D perturbation of the basic flow is also reported for comparison. The 2D perturbation has the same y shape as the optimal streak shape in the middle of the absolute region ($x = 2.7$) but is uniform instead of periodic in the spanwise direction. For this 2D perturbation, A_0 is unambiguously defined and A_s is defined as the maximum associated ΔU taken at $x = 2.7$.

From the figures it is clearly seen how the first order sensitivities ds_r/dA_0 and ds_r/dA_s computed for $A_0 = A_s = 0$ are zero for the 3D perturbations and non-zero for the 2D perturbations as predicted by the first order sensitivity analysis. According to a first-order sensitivity analysis one would expect the 2D perturbations to be more effective than 3D ones in quenching the global instability, but exactly the opposite is observed. Indeed, 2D perturbations are more effective than 3D ones in reducing s_r only for very small perturbation amplitudes, while the opposite is observed for larger amplitudes where the higher order dependence of s_r on A_0 and A_s induces more important reductions of s_r. We indeed find that 3D perturbations stabilize the global mode at a value of $A_s(x = 2.7)$ more than five times smaller, and more than ten times smaller in terms of A_0. A higher efficiency of 3D perturbations was expected for results expressed in terms of A_0, due to the gain associated with the lift-up of the 3D optimal perturbations. However, such a result was somehow unexpected when expressing the growth rate reductions in terms of A_s.

D. Nonlinear simulations

Non-linear simulations of the full Navier-Stokes equations have finally been performed to assess the effect of the inflow forcing of 3D optimal perturbations in the nonlinear regime. The same grid used in linear simulations has been used in the nonlinear ones. In a first simulation, the permanent harmonic self-sustained state supported by the reference 2D wake is allowed to develop. This 2D (spanwise uniform) self-sustained state is then given as an initial condition to simulations in the presence of the optimal perturbations (streaky wakes) of increasing amplitude. As expected from the linear analysis, the global perturbation kinetic energy E' associated to the self-sustained oscillations in the wake is reduced when the amplitude of the enforced optimal perturbations is increased (see Fig. 9). A stable steady streaky wake is found for case E, where the oscillations are completely suppressed.

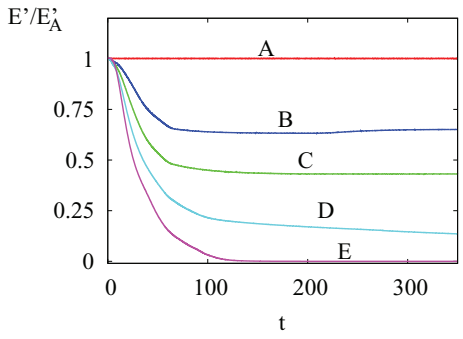

FIG. 9. Temporal evolution $E'(t)$ of the total perturbation kinetic energy, integrated over the whole computational box, supported by the streaky wakes, normalized to the E'_A of the reference 2D wake. The results are issued from nonlinear simulations where the permanent periodic state supported by the reference 2D wake is given as initial condition. In the presence of optimal perturbations of increasing amplitude, the amplitude of self-sustained oscillations is initially reduced (cases B, C, D), up to their complete suppression (case E).

Snapshots of the perturbation streamwise velocity in the $y = 0$ plane are reported in Fig. 10 for all the considered cases. For the reference 2D wake (case A), the self-sustained state is spanwise uniform (2D) with structures corresponding to standard von Kármán vortices. These vortical structures become increasingly modulated in the spanwise direction for increasing amplitudes A_0 of the forcing. Unsteady structures are completely suppressed for case E, where the basic flow streamwise streaks remain the only visible structures in the wake.

VI. SUMMARY AND DISCUSSION

In this study the optimal amplifications supported by an "artificial" non-parallel unstable 2D wake have been computed and their influence on the stability of the wake have been investigated by a global stability analysis. The main results can be summarized as follows:

- The energy of steady, symmetric spanwise periodic streamwise vortices forced at the inflow boundary can be significantly amplified downstream leading to large amplitude varicose streamwise streaks.
- An increase of the spanwise wavelength λ_z of the perturbations leads to larger energy amplification and to taller (in y) optimal structures.
- The used optimization technique, based on the simulation of the responses to a set of linearly independent inflow forcings, has proved very flexible. Only 16 simulations of independent forcings were needed to obtain accuracies higher than 1% on the optimal energy growths.
- The unstable global mode of the reference 2D wake at $Re = 50$ is completely stabilized when optimal inflow perturbations (vortices) are forced with sufficiently large amplitude.
- The results of first order local sensitivity analyses[10,11] are easily extended to the non-parallel case to show that the sensitivity of the 2D global mode eigenvalue to 3D spanwise periodic modifications of the basic flow is zero, while it is in general non-zero for 2D modifications.
- 3D optimal perturbations require smaller amplitudes than a reference 2D forcing to quench the global instability, and this both in terms of *rms*-amplitude of the inflow forcing and in terms of the basic flow distortion amplitude measured in the centre of the absolute instability region of the reference 2D wake. This is in contrast with the prediction of the sensitivity analysis.

The trends observed for the optimal energy amplification and the associated optimal perturbations in the non-parallel case are in qualitative agreement with those found in the local stability analysis.[12] In particular, the shapes of the optimal inputs (streamwise vortices) and those of the optimal outputs (streamwise streaks) are very similar for both analyses. When comparing the results, care must however be exerted in, e.g., selecting the appropriate spanwise wavenumbers to compare, as the local dimensionless wavenumber keeps increasing while going downstream in the non-parallel wake. Using the wavenumber made dimensionless with respect to the inflow reference length, the

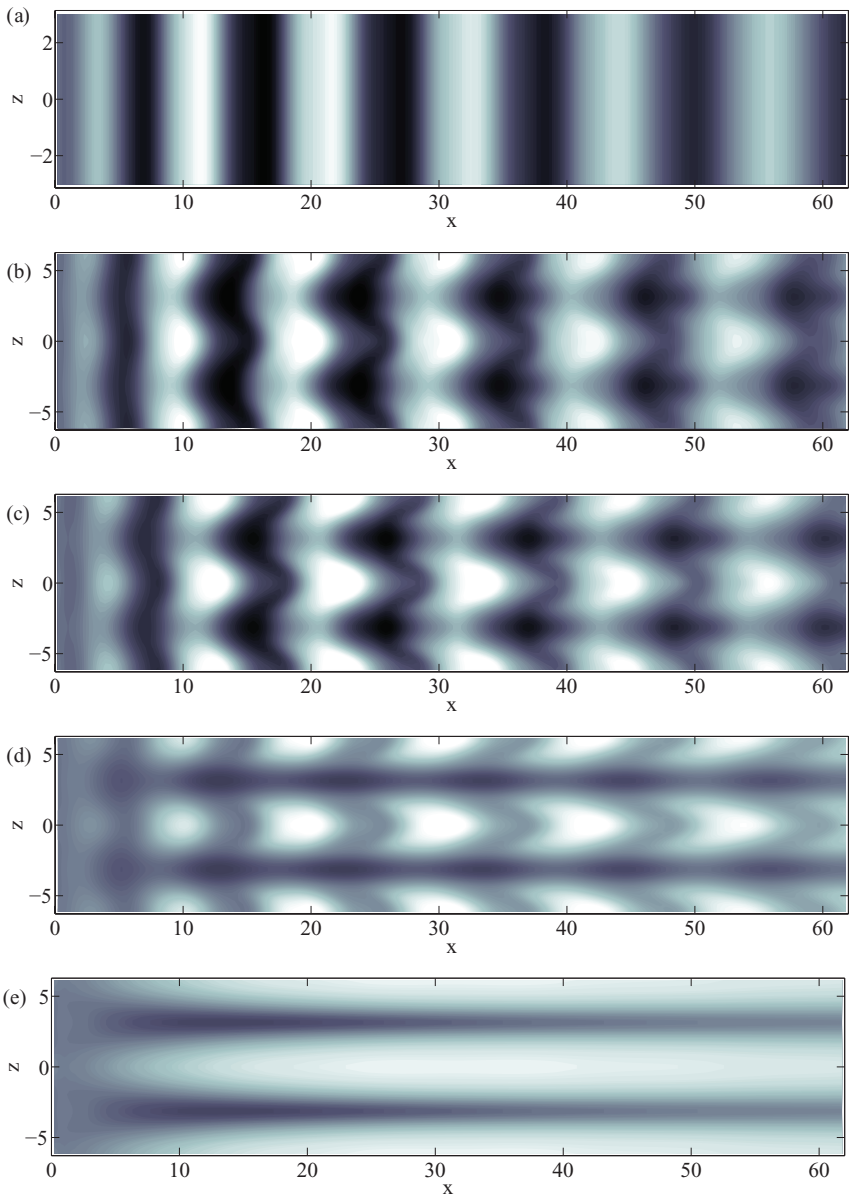

FIG. 10. Snapshots from fully nonlinear simulations. Streamwise perturbation velocity $u'(x, y = 0, z) = u(x, y = 0, z) - U_{2D}(x, y)$ in the $y = 0$ symmetry plane in the permanent regime ($t = 250$). The reference 2D case A is reported in panel (a), while cases B, C, D, and E, obtained by increasing the amplitude A_0 of the inflow optimal perturbations, are reported in panels (b) to (e) (top to bottom). Case A displays self-sustained periodic oscillations of 2D structures in the wake. These structures become increasingly 3D and of smaller *rms* value for increasing values of the enforced A_0 (cases B to D). The oscillations are completely suppressed in case E where the stable streaky basic flow is observed after transients are extinguished.

growths in the non-parallel wake appear smaller than the ones that would be predicted by keeping the wake frozen and parallel.

The fact that the linear global instability can be suppressed by optimal spanwise perturbations is in agreement with the idea that these 3D perturbations efficiently reduce the local absolute growth in the wave-maker region of the flow.[10,12] It also extends to flows with an "oscillator" dynamics[3,21] the control strategy based on the forcing of optimally amplified streaks that has been successfully used to stabilize convectively unstable waves in non-parallel boundary layers.[23–26] In this type of control strategy, optimal vortices are forced which then efficiently generate the streaks leading *in fine* to

the stabilization. This control technique is much more efficient than directly forcing the stabilizing streaks because the lift-up effect is used as an amplifier of the control action. Otherwise, much larger forcing amplitudes would be required to directly force the streaks.

The conclusions concerning the sensitivity analysis are, we believe, probably the most relevant of this study. According to a first order sensitivity analysis, the 3D spanwise periodic forcing or modification of the basic flow with amplitude A is less effective than a 2D one with the same amplitude because the sensitivity of 3D perturbations is zero (growth rate reductions $\sim A^2$, with zero derivative in $A = 0$), while the 2D sensitivity is not zero (growth rate reductions $\sim A$). While these conclusions are correct for very small amplitudes A of the basic flow modifications, they are not correct for larger amplitudes where the parabola-shaped growth rate reductions (3D control) have grown larger than the straight line ones (2D control). In our specific case this cross-over happens at very small amplitudes of the forcing, of the order of 1/10 of the amplitude required for stabilization by 3D modifications and of the order of 1/100 of the one required by 2D modifications. Considering that these results have been obtained at a Reynolds number only 20% above the critical value for global instability, this means that except in very weakly unstable situations, where small control amplitudes suffice to stabilize the perturbations, a first order sensitivity leads to misleading conclusions when the stabilizing efficiency of 3D and 2D perturbations is compared.

An important question, left for future study, is how to force optimal perturbations in the presence of the bluff body. As already mentioned, many ways to modulate wakes in the spanwise direction have been already implemented, among which, the sinusoidal indentation of the leading and/or the trailing edge of the body,[4–7] and the spanwise periodic blowing and suction at the wall surface.[8] The achieved wake modulations are strikingly similar to the streaky wakes investigated in the present study, suggesting that, just like in boundary layers, the optimal streaks represent a sort of "attractor" of the spanwise modulated solutions. However, it is not clear which of these strategies, if any, predominantly uses vortices to force the streaks instead of directly forcing the streaks. It would also be interesting to investigate the optimal amplification and the control efficiency of periodic inflow perturbations. Additional work is granted on these issues.

ACKNOWLEDGMENTS

G.D.G. acknowledges the support of ANRT via the convention CIFRE 742/2011.

APPENDIX: NUMERICAL SIMULATIONS

The Navier-Stokes equations (nonlinear and linearized) have been numerically integrated using *OpenFoam*, an open-source finite volumes code (see http://www.openfoam.org). The flow is solved inside the domain $[0, L_x] \times [-L_y/2, L_y/2] \times [0, L_z]$ that is discretized using a grid with N_x and N_z equally spaced points in the streamwise and spanwise directions, respectively. N_y points are used in the y direction using stretching to densify points in the region where the basic flow shear is not negligible. The fractional step, pressure correction PISO (Pressure Implicit with Splitting of Operators) scheme is used to advance the solutions in time.

TABLE II. Numerical grids used for the computation of optimal perturbations. As a y-symmetry is enforced the equations are solved only in the $[0, L_y/2]$ half-domain.

β	L_z	Nz	$Ly/2$	Ny	Lx	Nx
0.5	12.57	48	20	120	124	300
0.75	8.38	48	20	120	124	300
1	6.28	24	10	80	124	300
1.25	5.03	24	10	80	124	300
1.5	4.20	12	10	80	124	300
1.75	3.60	12	10	80	124	300

Different grids have been used to compute optimal linear perturbations of different spanwise wavenumbers, as reported in Table II.

Nonlinear streaky basic flows for $\beta = 1$ have been computed using the same grid used for the computation of the linear optimals at the same β. For the linear and nonlinear simulations of the perturbations to the 3D streaky basic flows, however, the domain is doubled in the y direction ($[-L_y/2, L_y/2]$ instead of $[0, L_y/2]$) as the y symmetry is no more enforced. Te box is also doubled in the spanwise direction ($L_z = 2\lambda_z$) in order to include subharmonic perturbations. The corresponding N_y and N_z are also doubled leading to a grid with $L_x = 124$, $L_y/2 = 10$, $L_z = 4\pi$, $N_x = 300$, $N_y = 160$, $N_z = 48$ with $\Delta x = 0.4$, $\Delta z = 0.26$ and a minimum $\Delta y = 0.01$ on the symmetry axis and a maximum $\Delta y = 0.1$ near the freestream boundary.

[1] J. M. Chomaz, P. Huerre, and L. G. Redekopp, "Bifurcations to local and global modes in spatially developing flows," Phys. Rev. Lett. **60**, 25–28 (1988).
[2] P. Monkewitz, "The absolute and convective nature of instability in two-dimensional wakes at low Reynolds numbers," Phys. Fluids **31**, 999–1006 (1988).
[3] P. Huerre and P. A. Monkewitz, "Local and global instabilities in spatially developing flows," Annu. Rev. Fluid Mech. **22**, 473–537 (1990).
[4] M. Tanner, "A method of reducing the base drag of wings with blunt trailing edges," Aeronaut. Q. **23**, 15–23 (1972).
[5] N. Tombazis and P. Bearman, "A study of three-dimensional aspects of vortex shedding from a bluff body with a mild geometric disturbance," J. Fluid Mech. **330**, 85–112 (1997).
[6] P. Bearman and J. Owen, "Reduction of bluff-body drag and suppression of vortex shedding by the introduction of wavy separation lines," J. Fluids Struct. **12**, 123–130 (1998).
[7] R. M. Darekar and S. J. Sherwin, "Flow past a square-section cylinder with a wavy stagnation face," J. Fluid Mech. **426**, 263–295 (2001).
[8] J. Kim and H. Choi, "Distributed forcing of flow over a circular cylinder," Phys. Fluids **17**, 033103 (2005).
[9] H. Choi, W. Jeon, and J. Kim, "Control of flow over a bluff body," Annu. Rev. Fluid Mech. **40**, 113–139 (2008).
[10] Y. Hwang, J. Kim, and H. Choi, "Stabilization of absolute instability in spanwise wavy two-dimensional wakes," J. Fluid Mech. **727**, 346–378 (2013).
[11] Y. Hwang and H. Choi, "Control of absolute instability by basic-flow modification in a parallel wake at low Reynolds number," J. Fluid Mech. **560**, 465 (2006).
[12] G. del Guercio, C. Cossu, and G. Pujals, "Stabilizing effect of optimally amplified streaks in parallel wakes," J. Fluid Mech. **739**, 37–56 (2014).
[13] T. Ellingsen and E. Palm, "Stability of linear flow," Phys. Fluids **18**, 487 (1975).
[14] M. T. Landahl, "A note on an algebraic instability of inviscid parallel shear flows," J. Fluid Mech. **98**, 243–251 (1980).
[15] N. Abdessemed, A. Sharma, S. Sherwin, and V. Theofilis, "Transient growth analysis of the flow past a circular cylinder," Phys. Fluids **21**, 044103 (2009).
[16] X. Mao, H. Blackburn, and S. Sherwin, "Optimal inflow boundary condition perturbations in steady stenotic flow," J. Fluid Mech. **705**, 306–321 (2012).
[17] P. Andersson, M. Berggren, and D. Henningson, "Optimal disturbances and bypass transition in boundary layers," Phys. Fluids **11**, 134–150 (1999).
[18] P. Luchini, "Reynolds-number independent instability of the boundary layer over a flat surface. Part 2: Optimal perturbations," J. Fluid Mech. **404**, 289–309 (2000).
[19] P. Andersson, L. Brandt, A. Bottaro, and D. Henningson, "On the breakdown of boundary layers streaks," J. Fluid Mech. **428**, 29–60 (2001).
[20] A. Bottaro, P. Corbett, and P. Luchini, "The effect of base flow variation on flow stability," J. Fluid Mech. **476**, 293–302 (2003).
[21] J. M. Chomaz, "Global instabilities in spatially developing flows: Nonnormality and nonlinearity," Annu. Rev. Fluid Mech. **37**, 357–392 (2005).
[22] This is a simple consequence of the integration in z of the product of spanwise sinusoidal and of a spanwise uniform function, which is itself spanwise sinusoidal and whose spanwise integral is therefore zero.
[23] C. Cossu and L. Brandt, "Stabilization of Tollmien-Schlichting waves by finite amplitude optimal streaks in the Blasius boundary layer," Phys. Fluids **14**, L57–L60 (2002).
[24] C. Cossu and L. Brandt, "On Tollmien–Schlichting waves in streaky boundary layers," Eur. J. Mech. B **23**, 815–833 (2004).
[25] J. Fransson, L. Brandt, A. Talamelli, and C. Cossu, "Experimental study of the stabilisation of Tollmien-Schlichting waves by finite amplitude streaks," Phys. Fluids **17**, 054110 (2005).
[26] J. Fransson, A. Talamelli, L. Brandt, and C. Cossu, "Delaying transition to turbulence by a passive mechanism," Phys. Rev. Lett. **96**, 064501 (2006).